HHS Public Access

Author manuscript

Cell Rep. Author manuscript; available in PMC 2016 November 14.

Published in final edited form as:

Cell Rep. 2016 November 8; 17(7): 1764–1772. doi:10.1016/j.celrep.2016.10.031.

PF4 promotes platelet production and lung cancer growth

Ferdinando Pucci[1,π], **Steffen Rickelt**[2], **Andita P. Newton**[1], **Christopher Garris**[1,3], **Ernesto Nunes**[4], **Charles Evavold**[1,3], **Christina Pfirschke**[1], **Camilla Engblom**[1,3], **Mari Mino-Kenudson**[5], **Richard O. Hynes**[2], **Ralph Weissleder**[1,6,7], and **Mikael J Pittet**[1,6,*,¶]

[1]Center for Systems Biology, Massachusetts General Hospital Research Institute, Harvard Medical School, Boston, MA 02114, USA

[2]Howard Hughes Medical Institute, Koch Institute for Integrative Cancer Research, Massachusetts Institute of Technology, Cambridge, MA 02139, USA

[3]Graduate Program in Immunology, Harvard Medical School, Boston, MA 02115, USA

[4]Department of Computer Science and Engineering, University of Minnesota, Minneapolis, MN 55455, USA

[5]Department of Pathology, Massachusetts General Hospital, Boston, MA 02114, USA

[6]Department of Radiology, Massachusetts General Hospital, Boston, MA 02114, USA

[7]Department of Systems Biology, Harvard Medical School, MA 02115, USA

Summary

Co-option of host components by solid tumors facilitates cancer progression and can occur in both local tumor microenvironments and remote locations. At present, the signals involved in long-distance communication remain insufficiently understood. Here, we identify PF4 (platelet factor 4, CXCL4) as an endocrine factor whose over-expression in tumors correlates with decreased overall patient survival. Furthermore, engineered PF4 over-production in a Kras-driven lung adenocarcinoma genetic mouse model expanded megakaryopoiesis in bone marrow, augmented platelet accumulation in lungs and accelerated *de novo* adenocarcinogenesis. Additionally, anti-platelet treatment controlled mouse lung cancer progression, further suggesting that platelets can modulate the tumor microenvironment to accelerate tumor outgrowth. These findings support PF4 as a cancer-enhancing endocrine signal that controls discrete aspects of bone marrow hematopoiesis and tumor microenvironment and should be considered as a molecular target in anticancer therapy.

*Corresponding address: mpittet@mgh.harvard.edu.
πPresent address: Torque Therapeutics Inc., Cambridge, MA 02142, USA
¶Lead contact

Author contributions

FP and MJP conceived the research plan and wrote the manuscript. FP, SR, CG, CP, CEng, performed research and analyzed data. APN, CEva and MMK performed research. EN computer coded and analyzed data. ROH, RW and MJP analyzed data and supervised the work.

Graphical abstract

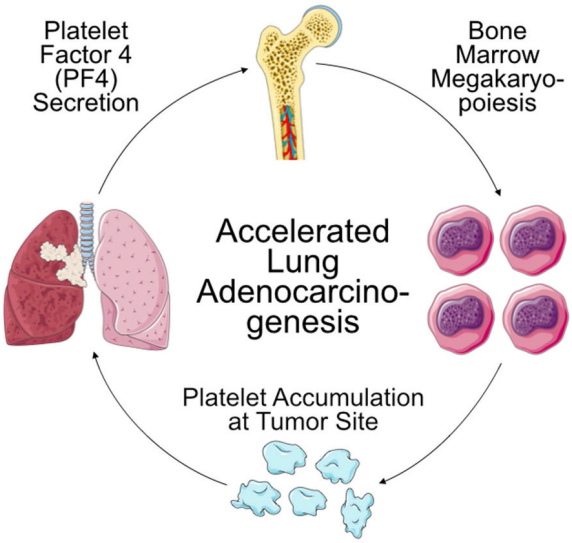

Introduction

Diverse tumor-associated host cells, including endothelial cells, fibroblasts and hematopoietic cells, are often locally co-opted by tumors to enable tumorigenesis or sustain tumor outgrowth (Hanahan and Coussens, 2012; Engblom et al., 2016). The study of the cellular and molecular mechanisms underlying the tumor microenvironment has generated not only new anticancer treatments, such as immuno- and antiangiogenic therapies, but also a new field of fundamental investigation centered on the ontogeny of tumor-infiltrating host cells (McAllister and Weinberg, 2014; Pittet et al., 2014). This research has discovered that growing tumors can continuously recruit new hematopoietic cells from the circulation by releasing signals that amplify the production of hematopoietic progenitors in remote hematopoietic organs. Long-range tumor-associated signals include osteopontin, a tumor-secreted endocrine factor that activates bone marrow cells (McAllister et al., 2008); G-CSF, a tumor-derived factor that promotes bone marrow myelopoiesis (Casbon et al., 2015) and Angiotensin-II, a peptide hormone that instigates extramedullary monocytopoiesis (Cortez-Retamozo et al., 2013). However, while local immune-neoplastic interactions in the microenvironment are well studied, several aspects of systemically activated tumor-associated immune components remain unclear.

Here we aimed to identify new candidate long-range communication signals involved in lung adenocarcinoma. We focused on this disease because it is the leading cause of cancer death (Torre et al., 2016) and because newly available high-throughput datasets allow us to interrogate this disease in both patients (Nguyen et al., 2009) and genetic mouse models that closely recapitulate the human disease (Taguchi et al., 2011). Initially, we developed a screening strategy that considered three defining properties of tumor-associated endocrine factors, namely: 1) their expression in tumors should be altered in both murine and human lung adenocarcinomas; 2) their changed expression should be associated with differences in patient survival; 3) their plasma concentration should be modified in lung adenocarcinoma-

bearing mice. Interrogating these phenotypes in both humans and mice enabled us to identify circulating factors that may be relevant to human disease and can be manipulated genetically to allow murine analyses of mechanisms and causality.

This strategy identified several factors, and of these, PF4 seemed the most prominent in lung cancer. We next performed deeper biological studies to identify whether systemically overexpressed PF4 instigates hematopoietic cell production away from the tumor stroma, instructs differentiation of defined hematopoietic cell types and alters the tumor microenvironment and tumorigenesis. To this end, we compared lung adenocarcinoma genetic mouse models that expressed *Pf4* at either low or high levels, and we genetically induced systemic PF4 production in mice that otherwise expressed this factor at low levels. In doing so we found PF4 to be responsible for stimulating discrete tumor-induced changes, namely megakaryocytic expansion in bone marrow and platelet accumulation at the tumor site. Furthermore, systemic PF4 production substantially accelerated Kras-driven tumorigenesis, a result that supports this factor as a tumor-promoting signal that connects lung tumors to distinct bone-marrow hematopoietic components.

Results

Identification of candidate long-range factors associated with altered patient survival

To identify previously unknown long-range communication signals involved in lung adenocarcinoma we screened *in silico* candidate long-range factors in Kras lung adenocarcinoma-bearing mice (Taguchi et al., 2011) and lung adenocarcinoma patients (Nguyen et al., 2009) (**Fig 1A**). By considering plasma proteins with significantly varied expression ($p<0.05$) in tumor-bearing mice, when compared to tumor-free littermates (Taguchi et al., 2011), we shortlisted 60 candidate factors, of which 33 were over-abundant and 27 were under-abundant (**Fig S1A**).

To assess these 60 factors in lung adenocarcinoma patients, we mined both tumor transcriptome profiles (at time of diagnosis) and survival data from 225 patients (Nguyen et al., 2009). Specifically, we compared the overall patient survival with highest (top 20%) and lowest (bottom 20%) mRNA expression levels for each candidate factor. Of the 33 over-abundant factors noted above, six were associated with altered patient survival ($p<0.05$ after Bonferroni correction): over-expression of three of them (*Pf4*, *Agt*, *Ppia*) correlated with decreased patient survival while overexpression of the remaining three (*Npc2*, *Sftpb*, *Slit2*) correlated with increased patient survival (**Fig 1B**). Of the 27 under-abundant factors noted above, five were associated with altered patient survival: under-expression of four of them (*Prg4*, *Rgn*, *Sepp1*, *Thumpd1*) correlated with decreased patient survival while under-expression of *Wdr62* correlated with increased patient survival (**Fig 1C**). Overall, this screening identified four candidate harmful factors (*Pf4*, *Agt*, *Ppia*, *Wdr62*) and seven candidate protective factors (*Npc2*, *Prg4*, *Rgn*, *Sepp1*, *Sftpb*, *Slit2*, *Thumpd1*) in lung adenocarcinoma. Thus 11 of the initial 60 candidates were associated with altered overall patient survival. For comparison, when assessing 60 randomly selected genes we found that only 2.6 ± 0.2 (mean ± SEM, n = 60 iterations) of them were associated with differences in patient survival. Consequently, seeding our screening with cancer-associated endocrine

factors significantly increased the chance that such candidates were also associated with survival changes (11 compared to 2.6 ± 0.2; $p < 0.0001$).

To further test the harmful and protective candidate factors identified above, we evaluated whether their transcript levels were altered at the tumor site in lung adenocarcinoma models driven by either oncogenic Kras only (*Kras*^{G12D}, hereafter referred to as K) or oncogenic Kras and p53 deletion (*Kras*^{G12D};*p53*$^{fl/fl}$, hereafter referred to as KP). We used these two genetic models because they both carry mutations frequently found in human lung adenocarcinoma (*KRAS* and *TP53* are mutated in ~25% and ~50%, of patients, respectively) but may co-opt the host immune response differently and produce different protective and harmful factors. Cre-expressing adenoviruses were introduced intranasally into K or KP mice to enable Cre delivery to lung epithelial cells and allow tumors to arise in the tissue (DuPage et al., 2009). We assayed intratumoral mRNA expression levels when tumor burden was similar in both models (**Fig S1B**), i.e. at week 20 for K mice and at week 11 for KP mice. Our assay also included tumor-free lungs as control tissue. Two of seven harmful candidate genes (*Pf4 and Agt*) and two of four protective candidate genes (*Npc2* and *Sftpb*) were significantly overexpressed in KP tumors; *Sftpb* was also overexpressed in K tumors (**Fig 1D**). The candidate protective factor *Prg4* was under-expressed in K mice (**Fig 1E**).

PF4 as a candidate lung adenocarcinoma-promoting factor

Of the harmful candidate factors identified above, we sought to further interrogate PF4 because it was most highly (~30-fold) over-expressed in KP nodules when compared to K nodules and tumor-free lungs (**Fig 1D**). Also, PF4 levels in circulation and within tumors have been associated with increased tumor growth (Poruk et al., 2010) but whether PF4 causally affects tumor development has remained unknown. Additionally, defining whether and how PF4 impacts distant organs and/or plays a role in tumor-host communication required study. Our initial data indicated a strong association between *PF4* overexpression and tumor development based on increased circulating PF4 plasma levels in Kras-driven lung tumor models (**Fig S1A**) and decreased overall survival in patients with high *PF4* expression in tumor nodules (**Fig 1B**). The latter finding was confirmed using independent lung adenocarcinoma datasets from 665 patients (Director's et al., 2008) (**Fig S1C**). Also, statistical analysis of demographic data from the two cohorts of patients identified based on *PF4* expression levels in tumors (i.e. *PF4*^{HI} and *PF4*^{LO} patients) did not identify a bias that could explain the underlying difference in survival (**Fig S1D**).

In subsequent experiments, we genetically augmented systemic PF4 production in K mice, which were otherwise poor *Pf4* expressers (**Fig 1D**), and asked whether this change was sufficient to induce discrete alterations in hematopoietic tissues and the tumor microenvironment that could foster tumor progression. To increase systemic PF4 levels in K mice, we created a lentiviral vector (PF4-LV) containing the native murine *Pf4* coding sequence under the strong constitutive promoter/enhancer *hEF1a* (**Fig 2A**) and injected concentrated PF4-LV preparations intravenously to transduce liver cells *in vivo*. A lentiviral vector lacking the *Pf4* expression cassette was used as control (Ctrl-LV) (**Fig S2A**). We excluded marker genes in both vectors to avoid immune clearance of transduced cells (Brown et al., 2006). Liver cells obtained from PF4-LV-treated K mice on week eight post

LV injection secreted ~1.3-1.5 times more PF4 than those from either Ctrl-LV-treated K mice or tumor-free control mice (**Fig 2B**). Furthermore, vector copy number in liver cells remained detectable at week eight, suggesting that PF4-producing cells were not cleared by the host immune system (**Fig S2B**). These results indicated the possibility of modulating the expression of a candidate systemic factor and testing its impact on the host and tumor progression in mice.

Systemic PF4 selectively expands the bone marrow megakaryocyte lineage

To assess PF4's impact on host responses to lung cancer, we induced *de novo* carcinogenesis in K mice by intranasally administering Cre-expressing adenoviral vectors. Next, we instigated systemic PF4 production at week nine by delivering PF4-LV intravenously and then analyzed hematopoietic cells in various tissues at week 17 (**Fig 2C**). PF4-LV-treated K mice showed significantly increased cellularity in the bone marrow but not in the spleen, when compared to Ctrl-LV-treated K mice (**Fig 2D**); this distinguishes PF4 from AGT, which instead selectively increases splenic cellularity (Cortez-Retamozo et al., 2013).

We then examined PF4's impact on bone marrow hematopoietic stem and progenitor cells and more mature immune cell lineages. We compared PF4-LV-treated and Ctrl-LV-treated K mice as mentioned above, as well as unmanipulated KP mice since their tumors naturally overexpressed *Pf4* (**Fig 1D**). In comparison to Ctrl-LV-treated K mice, KP mice contained more hematopoietic stem and progenitor cell populations (**Fig 2E** and **Fig S2C**), including long-term hematopoietic stem cells (LT-HSCs), multipotential progenitors (MPPs), common lymphoid progenitors (CLPs), granulocyte/macrophage progenitors (GMPs), macrophage/dendritic cell progenitors (MDPs)and megakaryocyte progenitors (MKPs). KP mice also showed more mature bone-marrow immune cell lineages including monocytes, neutrophils and megakaryocytes (**Fig 2F**).

By contrast, PF4-LV-treatment in K mice instigated a narrower blood lineage alteration. Among hematopoietic stem and progenitor cell populations, PF4-LV-treated K mice selectively expanded CMPs and MKPs when compared to Ctrl-LV treated K mice, while LT-HSCs, MPPs, CLPs, GMPs and MDPs remained detectably unchanged (**Fig 2E**). Additionally, PF4-LV-infected K mice showed increased bone marrow megakaryocytes, but neither monocytes nor neutrophils (**Fig 2F**). As expected, PF4-LV-treated K mice did not have more hematopoietic stem and progenitor cells in the spleen (**Fig S2D**). These findings indicate that systemic PF4 over-expression specifically mediates a bone marrow megakaryopoietic response (CMPs→MKPs→megakaryocytes; **Fig 2G**).

PF4 increases platelet accumulation in tumor-bearing lungs

Based on PF4's impact on bone marrow megakaryopoiesis, we reasoned that this factor may influence the tumor microenvironment by increasing platelet accumulation. Initially, we validated a monoclonal antibody (mAb) against mouse platelet glycoprotein Ib alpha chain CD42b (**Fig S3A-B**). We then stained lung histology sections from PF4-LV- and Ctrl-LV-treated K mice as well as KP mice (**Fig 3A**), double-blind quantified by mCD42b signal (**Fig 3B**). This analysis identified increased $CD42b^+$ platelet cluster accumulation in the lungs of

PF4-LV-treated mice. As expected, KP tumor-bearing lungs showed high $CD42b^+$ platelet cluster accumulation (**Fig 3A-B**).

Additional *ex vivo* flow cytometry-based analysis revealed that the abundance of other immune cell types remained unchanged in the lungs of PF4-LV-treated K mice as compared to their Ctrl-LV-treated counterparts (**Fig 3C** and **Fig S3C**). These data confirm that PF4 selectively amplified the megakaryocyte lineage in the bone marrow without affecting the lymphoid cell and phagocyte lineages. The selective change in platelet accumulation at the tumor site indicates PF4 drives this phenotype directly (as opposed to PF4 affecting other cells that would then recruit platelets to the tumor stroma).

To test whether the results detailed above had clinical correlates, we assessed platelet accumulation in lung adenocarcinoma patients. We used an anti-human CD42b mAb that, we confirmed, labels $CD45^-$ platelets and does not cross-react with other $CD45^+$ white blood cells (**Fig S3D**). We then assessed tumor infiltration by platelets in 29 tumor biopsy sections from NSCLC patients genotyped for *KRAS* and *TP53* mutations. *KRAS/TP53*-mutated tumors showed increased platelet infiltration when compared to *KRAS*- and *TP53*-mutated tumors and tumor-free tissue (**Fig 3D-E** and **Fig S3E**). Although the number of patients carrying both mutations was limited, these findings indicate that platelets efficiently accumulate in at least a fraction of human lung tumors and that the K and KP mouse models are relevant for studying tumors that share features with their human counterparts.

Platelets and circulating PF4 promote Kras-driven lung adenocarcinogenesis

Treatment of KP tumor-bearing mice with clopidogrel, an inhibitor of platelet aggregation and activation (Quinn and Fitzgerald, 1999), reduced cancer growth as characterized by decreased lung weight (**Fig 4A**) and lung tumor burden (**Fig 4B-C**). Clopidogrel-treated mice, but not the PBS-treated controls, also maintained their overall body weight (**Fig S4A**) during the course of the experiment. These results indicate that platelets enhance KP tumor growth.

Conversely, we asked whether systemically increased PF4 production accelerates *de novo* lung tumor progression in K mice. Indeed, we found increased lung weights in PF4-LV-treated K mice as compared to their Ctrl-LV-treated counterparts (**Fig 4D**). We also generated whole-lung histological sections to evaluate whether PF4-LV-treated K mice's heavier lungs were due to higher tumor burden (**Fig 4E**). Quantified tumor area in these sections confirmed elevated tumor burden in PF4-LV-treated compared to control mice (**Fig 4F**). We also noted more tumor foci in PF4-LV mice than in their Ctrl-LV counterparts (**Fig 4G**). Together, these results provide *in vivo* evidence that increased systemic PF4 levels accelerate K tumor progression. PF4 did not accelerate K tumor growth in isolation *in vitro* (**Fig S4B**), further indicating that increased PF4 production fosters tumor growth by acting on host cell components.

Discussion

By cross-analyzing selected datasets from human and mouse lung adenocarcinomas, we identified candidate factors that may act as endocrine signals in tumor–host communication.

Furthermore, by manipulating systemic PF4 production, we validated this factor as a key constituent that alters discrete components of the tumor-associated host response and accelerates adenocarcinogenesis. Previous studies indicated that PF4 in steady-state suppresses megakaryopoiesis (Lambert et al., 2007; Oda et al., 2003) and induces hematopoietic stem cell quiescence (Bruns et al., 2014; Zhao et al., 2014) but can promote hemopoiesis and megakaryopoiesis under stress conditions such as radiotherapy or chemotherapy (Aidoudi et al., 1996; Bruns et al., 2014; Caen et al., 1999). Here, in the context of cancer, we found a causal link between increased endogenous PF4 levels and i) expanded megakaryopoiesis; ii) platelet accumulation in cancer-developing lungs; iii) accelerated tumor growth. That PF4 triggers these phenotypes during carcinogenesis accords with our understanding that cancer puts chronic stress on the hematopoietic system (Shalapour and Karin, 2015).

PF4-induced platelet accumulation in tumors is important because platelets can modulate tumor cells and the tumor microenvironment to accelerate cancer outgrowth. For example, platelets can promote tumor angiogenesis (Ho-Tin-Noé et al., 2008; Kuznetsov et al., 2012; Qi et al., 2015; Gebremeskel et al., 2015; Mezouar et al., 2015), prevent tumor cell recognition by natural killer cells (Nieswandt et al., 1999; Palumbo et al., 2005; Placke et al., 2012) and foster metastasis by recruiting myeloid cells into metastatic niches (Gay and Felding-Habermann, 2011; Labelle et al., 2014). Here we provide evidence for a direct role of PF4 in platelet accumulation in lung tumors, both in mouse models and patients.

PF4 analogs or fragments can be anti-angiogenic and by extension exert antitumor activities (Giussani et al., 2003; Maione et al., 1991; Tanaka et al., 1997). However, increased circulating native PF4 levels are associated with human lung cancer (Taguchi et al., 2011; Engels et al., 2015). Importantly, in this study we used a *Pf4* expression cassette that produced native PF4 *in vivo*. With this approach we not only confirmed a positive association between native *Pf4* over-expression and faster tumor progression, but also identified PF4 as a causal factor driving this phenotype.

Systemically-increased PF4 production during *de novo* carcinogenesis selectively amplified medullary megakaryopoiesis and platelet accumulation at the tumor site. These findings indicate a specific control that is operated by tumors on the host and that extends beyond the local tumor microenvironment. KP tumors over-express several factors, including *Pf4* (as per this study) and *Agt* (Cortez-Retamozo et al., 2013), yet PF4's effects on medullary megakaryopoiesis were distinct from those of AGT (the Angiotensin II precursor) on extramedullary monocytopoiesis. Consequently, we propose that lung tumors can remotely control distinct hematopoietic cells by producing different endocrine factors. These factors (PF4, Angiotensin II, and likely others) shape the tumor microenvironment, consequently alter tumor progression and may thus be promising molecular targets for anticancer therapy.

Experimental Procedures

Mice

$Kras^{LSL-G12D/+};p53^{fl/fl}$ (referred to as KP) and $Kras^{LSL-G12D/+}$ (referred to as K) mice in a 129/j background were used as conditional mouse models of lung adenocarcinoma as

described previously (Cortez-Retamozo et al., 2012). All animal experiments were approved by the Massachusetts General Hospital Subcommittee on Research Animal Care. Methods to induce lung adenocarcinoma in these mice are described in Supplemental Experimental Procedures.

Human Tumor Samples

Sections from paraffin-embedded lung resection biopsies (n=29) from NSCLC patients with known *KRAS* and *TP53* gene mutation status were obtained from the Department of Pathology at Massachusetts General Hospital. CD42b immunohistochemistry was performed and evaluated blindly as described in the Supplemental Experimental Procedures.

PF4 lentiviral vectors

Concentrated VSV.G-pseudotyped, third-generation LV stocks were produced and titered as described previously (De Palma and Naldini, 2002). Lentiviral vector copy per genome (CpG) was calculated by titering the concentrated LV on 293T cells. The CpG of genomic DNA standard curves and samples was determined using custom TaqMan assays specific for LVs (Applied Biosystems). LV were injected i.v. $2 \bullet 10^4$ ng p24/mouse in 50-200ul, depending on the infectivity.

Bioinformatics and Statistics

In silico analyses were performed in R. The initial list of murine candidates used to probe lung-cancer patient microarray dataset was sequentially transformed from a list of murine proteins into: 1) their human orthologs; 2) their gene symbols; 3) the corresponding microarray probe IDs. The list of microarray probes was matched with human datasets for survival analysis, which used the log-rank test. GraphPad Prism 6 was used for all statistical analyses. Statistical tests for multivariate analyses were performed using 2-way ANOVA followed by Holm-Sidak multiple comparison test. P values were considered significant at < 0.05.

Gene and protein nomenclature

Capitalization of gene and protein symbols is styled according to species. For example, human gene symbol: *PF4*; Protein symbol: PF4. Mouse gene symbol: Pf4; Protein symbol: PF4.

Supplementary Material

Refer to Web version on PubMed Central for supplementary material.

Acknowledgements

This work was supported in part by the Samana Cay MGH Research Scholar Fund (to M.J.P.); NIH grants R21-CA190344, P50-CA86355 and R01-AI084880 (to M.J.P.), U54-CA126515 (to R.W.), U54-CA163109 (to R.O.H.) and F31-CA196035 (to C.G.); EMBO long-term fellowship and ECOR Funds for Medical Discovery Fellowship (to F.P.); Deutsche Forschungsgemeinschaft PF809/1-1 (to C.P.) and RI2408/1-1 (to S.R.); Metastasis/Cancer Research Postdoc fellowship from MIT Ludwig Center for Molecular Oncology Research (to S.R.); Boehringer Ingelheim Funds (to C.Eng); and the Howard Hughes Medical Institute (to R.O.H.). The authors thank the members of the Hope Babette Tang Histology Facility at the Koch Institute Swanson Biotechnology Center, Yoshiko Iwamoto of the Center for System Biology for technical support, and Dr. Wouter Meuleman for help with R coding.

References

Aidoudi S, Guigon M, Lebeurier I, Caen JP, Han ZC. In vivo effect of platelet factor 4 (PF4) and tetrapeptide AcSDKP on haemopoiesis of mice treated with 5-fluorouracil. Br J Haematol. 1996; 94:443–448. [PubMed: 8790139]

Brown BD, Venneri MA, Zingale A, Sergi Sergi L, Naldini L. Endogenous microRNA regulation suppresses transgene expression in hematopoietic lineages and enables stable gene transfer. Nat Med. 2006; 12:585–591. [PubMed: 16633348]

Bruns I, Lucas D, Pinho S, Ahmed J, Lambert MP, Kunisaki Y, Scheiermann C, Schiff L, Poncz M, Bergman A, Frenette PS. Megakaryocytes regulate hematopoietic stem cell quiescence through CXCL4 secretion. Nat Med. 2014; 20:1315–1320. [PubMed: 25326802]

Caen JP, Han ZC, Bellucci S, Alemany M. Regulation of megakaryocytopoiesis. Haemostasis. 1999; 29:27–40. [PubMed: 10494032]

Casbon AJ, Reynaud D, Park C, Gan DD, Schepers K, Passegué E, Werb Z. Invasive breast cancer reprograms early myeloid differentiation in the bone marrow to generate immunosuppressive neutrophils. Proc Natl Acad Sci U S A. 2015; 112:566–775. [PubMed: 25550509]

Cortez-Retamozo V, Etzrodt M, Newton A, Rauch PJ, Chudnovskiy A, Berger C, Ryan RJ, Iwamoto Y, Marinelli B, Gorbatov R, Forghani R, Novobrantseva TI, Koteliansky V, Figueiredo JL, Chen JW, Anderson DG, Nahrendorf M, Swirski FK, Weissleder R, Pittet MJ. Origins of tumor-associated macrophages and neutrophils. Proc Natl Acad Sci U S A. 2012; 109:2491–2496. [PubMed: 22308361]

Cortez-Retamozo V, Etzrodt M, Newton A, Ryan R, Pucci F, Sio SW, Kuswanto W, Rauch PJ, Chudnovskiy A, Iwamoto Y, Kohler R, Marinelli B, Gorbatov R, Wojtkiewicz G, Panizzi P, Mino-Kenudson M, Forghani R, Figueiredo JL, Chen JW, Xavier R, Swirski FK, Nahrendorf M, Weissleder R, Pittet MJ. Angiotensin II drives the production of tumor-promoting macrophages. Immunity. 2013; 38:296–308. [PubMed: 23333075]

De Palma M, Naldini L. Transduction of a gene expression cassette using advanced generation lentiviral vectors. Methods Enzymol. 2002; 346:514–529. [PubMed: 11883088]

Director's, Challenge Consortium for the Molecular Classification of Lung Adenocarcinoma. Shedden K, Taylor JM, Enkemann SA, Tsao MS, Yeatman TJ, Gerald WL, Eschrich S, Jurisica I, Giordano TJ, Misek DE, Chang AC, Zhu CQ, Strumpf D, Hanash S, Shepherd FA, Ding K, Seymour L, Naoki K, Pennell N, Weir B, Verhaak R, Ladd-Acosta C, Golub T, Gruidl M, Sharma A, Szoke J, Zakowski M, Rusch V, Kris M, Viale A, Motoi N, Travis W, Conley B, Seshan VE, Meyerson M, Kuick R, Dobbin KK, Lively T, Jacobson JW, Beer DG. Gene expression-based survival prediction in lung adenocarcinoma: a multi-site, blinded validation study. Nat Med. 2008; 14:822–827. [PubMed: 18641660]

DuPage M, Dooley AL, Jacks T. Conditional mouse lung cancer models using adenoviral or lentiviral delivery of Cre recombinase. Nat Protoc. 2009; 4:1064–1072. [PubMed: 19561589]

Engblom C, Pfirschke C, Pittet MJ. The role of myeloid cells in cancer therapies. Nat Rev Cancer. 2016; 16:447–62. [PubMed: 27339708]

Engels EA, Jennings L, Kemp TJ, Chaturvedi AK, Pinto LA, Pfeiffer RM, Trotter JF, Acker M, Onaca N, Klintmalm GB. Circulating TGF-β1 and VEGF and risk of cancer among liver transplant recipients. Cancer Med. 2015; 4:1252–1257. [PubMed: 25919050]

Gay LJ, Felding-Habermann B. Contribution of platelets to tumour metastasis. Nat Rev Cancer. 2011; 11:123–134. [PubMed: 21258396]

Gebremeskel S, LeVatte T, Liwski RS, Johnston B, Bezuhly M. The reversible P2Y12 inhibitor ticagrelor inhibits metastasis and improves survival in mouse models of cancer. Int J Cancer. 2015; 136:234–240. [PubMed: 24798403]

Giussani C, Carrabba G, Pluderi M, Lucini V, Pannacci M, Caronzolo D, Costa F, Minotti M, Tomei G, Villani R, Carroll RS, Bikfalvi A, Bello L. Local intracerebral delivery of endogenous inhibitors by osmotic minipumps effectively suppresses glioma growth in vivo. Cancer Res. 2003; 63:2499–2505. [PubMed: 12750272]

Hanahan D, Coussens LM. Accessories to the crime: functions of cells recruited to the tumor microenvironment. Cancer Cell. 2012; 21:309–322. [PubMed: 22439926]

Ho-Tin-Noé B, Goerge T, Cifuni SM, Duerschmied D, Wagner DD. Platelet granule secretion continuously prevents intratumor hemorrhage. Cancer Res. 2008; 68:6851–6858. [PubMed: 18701510]

Kuznetsov HS, Marsh T, Markens BA, Castaño Z, Greene-Colozzi A, Hay SA, Brown VE, Richardson AL, Signoretti S, Battinelli EM, McAllister SS. Identification of luminal breast cancers that establish a tumor-supportive macroenvironment defined by proangiogenic platelets and bone marrow-derived cells. Cancer Discov. 2012; 2:1150–1165. [PubMed: 22896036]

Labelle M, Begum S, Hynes RO. Platelets guide the formation of early metastatic niches. PNAS. 2014; 111:3053–61.

Lambert MP, Rauova L, Bailey M, Sola-Visner MC, Kowalska MA, Poncz M. Platelet factor 4 is a negative autocrine in vivo regulator of megakaryopoiesis: clinical and therapeutic implications. Blood. 2007; 110:1153–1160. [PubMed: 17495129]

Maione TE, Gray GS, Hunt AJ, Sharpe RJ. Inhibition of tumor growth in mice by an analogue of platelet factor 4 that lacks affinity for heparin and retains potent angiostatic activity. Cancer Res. 1991; 51:2077–2083. [PubMed: 1706960]

McAllister SS, Gifford AM, Greiner AL, Kelleher SP, Saelzler MP, Ince TA, Reinhardt F, Harris LN, Hylander BL, Repasky EA, Weinberg RA. Systemic endocrine instigation of indolent tumor growth requires osteopontin. Cell. 2008; 133:994–1005. [PubMed: 18555776]

McAllister SS, Weinberg RA. The tumour-induced systemic environment as a critical regulator of cancer progression and metastasis. Nat Cell Biol. 2014; 16:717–727. [PubMed: 25082194]

Mezouar S, Darbousset R, Dignat-George F, Panicot-Dubois L, Dubois C. Inhibition of platelet activation prevents the P-selectin and integrin-dependent accumulation of cancer cell microparticles and reduces tumor growth and metastasis in vivo. Int J Cancer. 2015; 136:462–475. [PubMed: 24889539]

Nguyen DX, Chiang AC, Zhang XH, Kim JY, Kris MG, Ladanyi M, Gerald WL, Massagué J. WNT/TCF signaling through LEF1 and HOXB9 mediates lung adenocarcinoma metastasis. Cell. 2009; 138:51–62. [PubMed: 19576624]

Nieswandt B, Hafner M, Echtenacher B, Männel DN. Lysis of tumor cells by natural killer cells in mice is impeded by platelets. Cancer Res. 1999; 59:1295–1300. [PubMed: 10096562]

Oda M, Kurasawa Y, Todokoro K, Nagata Y. Thrombopoietin-induced CXC chemokines, NAP-2 and PF4, suppress polyploidization and proplatelet formation during megakaryocyte maturation. Genes Cells. 2003; 8:9–15. [PubMed: 12558795]

Palumbo JS, Talmage KE, Massari JV, La Jeunesse CM, Flick MJ, Kombrinck KW, Jirousková M, Degen JL. Platelets and fibrin(ogen) increase metastatic potential by impeding natural killer cell-mediated elimination of tumor cells. Blood. 2005; 105:178–185. [PubMed: 15367435]

Pittet MJ, Nahrendorf M, Swirski FK. The journey from stem cell to macrophage. Ann N Y Acad Sci. 2014; 1319:1–18. [PubMed: 24673186]

Placke T, Örgel M, Schaller M, Jung G, Rammensee HG, Kopp HG, Salih HR. Platelet-derived MHC class I confers a pseudonormal phenotype to cancer cells that subverts the antitumor reactivity of natural killer immune cells. Cancer Res. 2012; 72:440–448. [PubMed: 22127925]

Poruk KE, Firpo MA, Huerter LM, Scaife CL, Emerson LL, Boucher KM, Jones KA, Mulvihill SJ. Serum platelet factor 4 is an independent predictor of survival and venous thromboembolism in patients with pancreatic adenocarcinoma. Cancer Epidemiol Biomarkers Prev. 2010; 19:2605–2610. [PubMed: 20729288]

Qi C, Li B, Guo S, Wei B, Shao C, Li J, Yang Y, Zhang Q, Li J, He X, Wang L, Zhang Y. P-Selectin-Mediated Adhesion between Platelets and Tumor Cells Promotes Intestinal Tumorigenesis in Apc(Min/+) Mice. Int J Biol Sci. 2015; 11:679–687. [PubMed: 25999791]

Quinn MJ, Fitzgerald DJ. Ticlopidine and clopidogrel. Circulation. 1999; 100:1667–1672. [PubMed: 10517740]

Shalapour S, Karin M. Immunity, inflammation, and cancer: an eternal fight between good and evil. J Clin Invest. 2015; 125:3347–3355. [PubMed: 26325032]

Taguchi A, Politi K, Pitteri SJ, Lockwood WW, Faca VM, Kelly-Spratt K, Wong CH, Zhang Q, Chin A, Park KS, Goodman G, Gazdar AF, Sage J, Dinulescu DM, Kucherlapati R, Depinho RA, Kemp

CJ, Varmus HE, Hanash SM. Lung cancer signatures in plasma based on proteome profiling of mouse tumor models. Cancer Cell. 2011; 20:289–299. [PubMed: 21907921]

Tanaka T, Manome Y, Wen P, Kufe DW, Fine HA. Viral vector-mediated transduction of a modified platelet factor 4 cDNA inhibits angiogenesis and tumor growth. Nat Med. 1997; 3:437–442. [PubMed: 9095178]

Torre LA, Siegel RL, Jemal A. Lung Cancer Statistics. Adv Exp Med Biol. 2016; 893:1–19. [PubMed: 26667336]

Zhao M, Perry JM, Marshall H, Venkatraman A, Qian P, He XC, Ahamed J, Li L. Megakaryocytes maintain homeostatic quiescence and promote post-injury regeneration of hematopoietic stem cells. Nat Med. 2014; 20:1321–1326. [PubMed: 25326798]

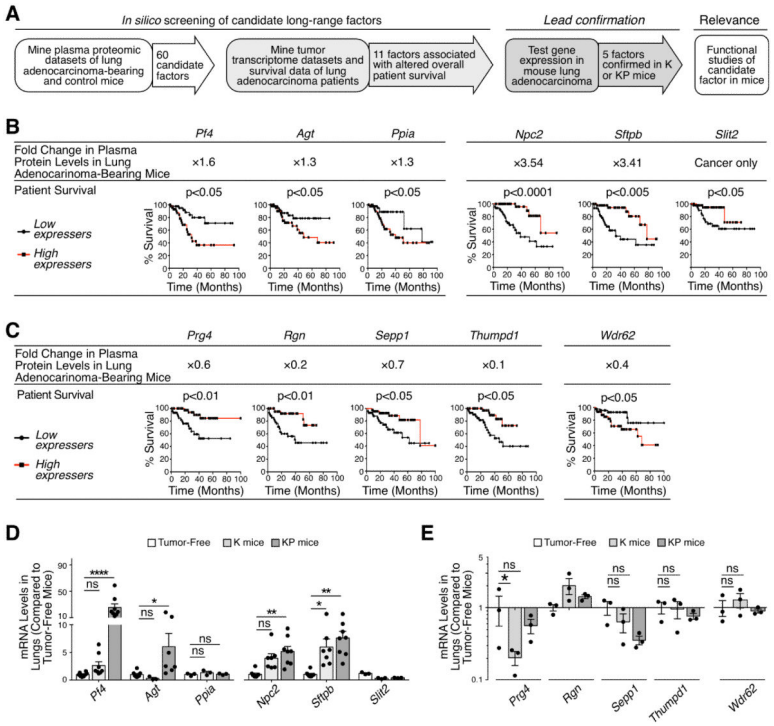

Figure 1. PF4 is a candidate long-range factor associated with altered survival in lung adenocarcinoma

(**A**) Workflow to identify candidate long-range endocrine signals involved in lung adenocarcinoma progression. The *in silico* screening employed a mouse proteomics dataset that cross-referenced a list of 60 candidate factors with patient microarray data to shortlist 11 factors associated with altered patient survival (left panels). Leads were tested experimentally in K and KP mice (middle panels) and one factor was selected for further functional studies (right panel).

(**B**) Identification of six factors over-abundant in plasma of lung adenocarcinoma-bearing mice as compared to tumor-free mice (top row) and whose over-expression was associated with decreased (Pf4, Agt and Ppia) or increased (Npc2, Sftpb and Slit) survival in lung adenocarcinoma patients (bottom row). Kaplan-Meier survival curves are shown for patients with highest (top 20%, n = 45) and lowest (bottom 20%, n = 45) mRNA expression levels for each factor.

(**C**) Identification of five factors under-abundant in plasma of lung adenocarcinoma-bearing mice as compared to tumor-free mice (top row) and whose over-expression is associated with improved (Prg4, Rgn, Sepp1 and Thumpd1) or decreased (Wdr62) survival in lung adenocarcinoma patients (bottom row). Kaplan-Meier survival curves are shown for patients with highest (top 20%, n = 45) and lowest (bottom 20%, n = 45) mRNA expression levels for each factor.

(**D-E**) mRNA levels in K and KP mouse lungs (as compared to tumor-free lungs) when tumor burden was similar in both models, i.e. at week 20 for K mice and at week 11 for KP mice. Candidate factors from panels **B** and **C** are shown in **D** and **E**, respectively. n = 3-8.

Results are expressed as mean ± SEM. *p < 0.05; **p < 0.01; ****p < 0.0001. Abbreviations are as follows: K, *Kras*^{G12D}; KP, *Kras*^{G12D};*p53*$^{fl/fl}$; ns, not significant; NSCLC, non-small cell lung cancer. See also Figure S1.

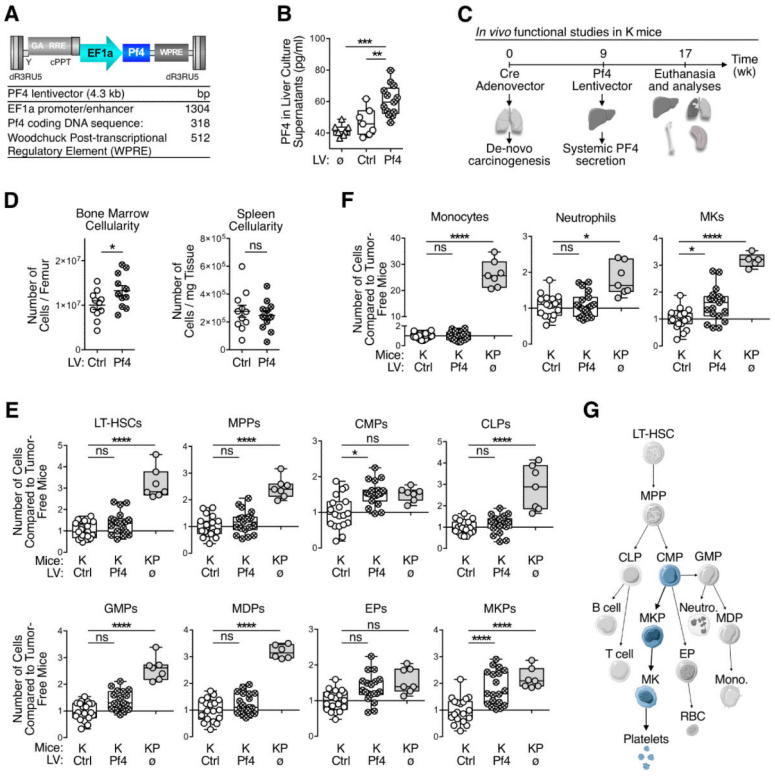

Figure 2. Systemic PF4 production selectively expands the bone marrow megakaryocyte lineage

(**A**) Schematics of PF4-LV features. Mouse native *Pf4* coding gene is constitutively expressed under a strong promoter, without any marker gene or tag that may elicit an immune rejection of PF4-over-expressing cells.

(**B**) ELISA for PF4 on total liver cell culture supernatants from tumor-free (ø), Ctrl-LV- and PF4-LV-treated K mice.

(**C**) Illustrated experimental design: K mice were dosed intranasally with adenoviral vectors expressing Cre to activate oncogenic Kras; after nine weeks, they received PF4-LV (or Ctrl-LV) intravenously to start systemic PF4 over-expression; at week 17 mice were euthanized and analyzed.

(**D**) Flow cytometry-based analysis of BM and spleen total viable cells from mice treated as in **C**.

(**E-F**) Flow cytometry-based analysis of BM hematopoietic stem/progenitor cells (**E**) and selected progeny (**F**) from mice treated as in **C**. KP mice were added as controls, since they natively over-express PF4 (See Fig. 1D).

(**G**) Cartoon depicting hematopoietic hierarchy and illustrating PF4-induced expansion of the megakaryopoietic lineage (in light blue).

Results are expressed as mean ± SEM. *p < 0.05; **p < 0.01; ****p < 0.0001.

Abbreviations are as follows: BM, bone marrow; CLP, common lymphoid progenitors; CMP, common myeloid progenitors; Ctrl, control; EP, erythroid progenitors; GMP, granulocyte-macrophage progenitors; K, $Kras^{G12D}$; KP, $Kras^{G12D};p53^{fl/fl}$; LT-HSC, long-term hematopoietic stem cells; LV, lentivector; MDP, monocyte-dendritic cell progenitors; MK, megakaryocyte; MKP, megakaryocyte progenitors; MPP, multi-potent progenitors; ns, not significant; RBC, red blood cell. See also Figure S2.

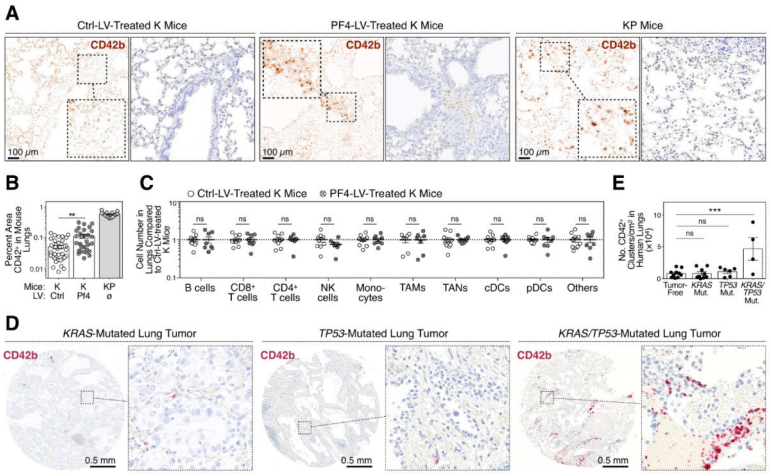

Figure 3. Systemic PF4 production amplifies platelet accumulation at the tumor site

(**A**) Immunohistochemistry staining for mCD42b (dark brown) on lung sections from K mice treated with either Ctrl- or PF4-LV, and from KP mice. Left panels show mCD42b signal (split brown channels), whereas right panels show original DAB staining (brown) with hematoxylin counterstain (blue). Scale bars represent 100 μm.

(**B**) Quantification of percent mCD42b+ areas per field of views, based on immunohistochemistry staining shown in **A**.

(**C**) Flow cytometry-based quantification of various immune cell types in the lungs of K mice treated with either Ctrl- or PF4-LV.

(**D**) Immunohistochemistry staining for hCD42b (red) on lung cancer patient tissue microarrays. Representative biopsies of *KRAS*-mutated (left), *TP53*-mutated (center) and both *KRAS*- and *TP53*-mutated tumors (right) are shown. Scale bars represent 0.5 mm.

(E) Quantification of hCD42b+ clusters per cm^2 based on immunohistochemistry staining shown in **D**.

Results are expressed as mean ± SEM. **p < 0.01; ***p < 0.001. Abbreviations are as follows: cDC, classical dendritic cell; ctrl, control; K, $Kras^{G12D}$; KP, $Kras^{G12D};p53^{fl/fl}$; LV, lentivector; mut. mutant; mono., monocyte; mutant; NK, natural killer; ns, not significant; pDC, plasmacytoid dendritic cell; TAM, tumor-associated macrophage; TAN, tumor-associated neutrophil. See also Figure S3

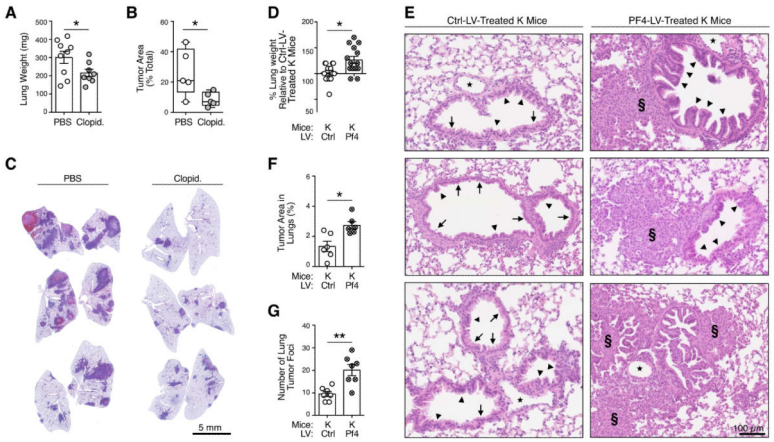

Figure 4. Platelets and systemic PF4 production promote cancer progression

(**A**) Lung weight of PBS-treated and clopidogrel-treated tumor-bearing mice 5 weeks after KP1.9 lung tumor cell injection.

(**B**) Histochemistry-based quantification of total tumor areas (as percentage of total lung section areas) in PBS- and clopidogrel-treated KP1.9 tumor bearing mice.

(**C**) Representative hematoxylin and eosin images of lung sections from the same mice as in **B**.

(**D**) Lung weight of Ctrl-LV- and PF4-LV-treated K mice 17 weeks after tumor initiation. Data shown as percentage of Ctrl-LV lung weight.

(**E-F**) Histochemistry-based quantification of total tumor areas (as percentage of total lung section areas) (**E**) and lung tumor foci (**F**) in Ctrl-LV- and PF4-LV-treated K mice.

(**G**) Representative hematoxylin and eosin images of lung sections from the same mice as in **A**. ⋆: blood vessels; →: normal epithelia; ▲: hyperplasia; §: adenoma. Scale bars represent 100 μm. Results are expressed as mean ± SEM. *p < 0.05; **p < 0.01. Abbreviations are as follows: Clopid, clopidogrel; Ctrl, control; K, *Kras*^{G12D}; LV, lentivector. See also Figure S4.